Resolution of Conformational States of *Dictyostelium* Myosin II Motor Domain Using Tryptophan (W501) Mutants: Implications for the Open-Closed Transition Identified by Crystallography†

András Málnási-Csizmadia, Robert J. Woolley, and Clive R. Bagshaw*

Department of Biochemistry, University of Leicester, Leicester LE1 7RH. U.K.

Received May 17, 2000; Revised Manuscript Received October 18, 2000

ABSTRACT: When myosin interacts with ATP there is a characteristic enhancement in tryptophan fluorescence which has been widely exploited in kinetic studies. Using *Dictyostelium* motor domain mutants, we show that W501, located at the end of the relay helix close to the converter region, responds to two independent conformational events on nucleotide binding. First, a rapid isomerization gives a small fluorescence quench and then a slower reversible step which controls the hydrolysis rate (and corresponds to the open-closed transition identified by crystallography) gives a large enhancement. A mutant lacking W501 shows no ATP-induced enhancement in the fluorescence, yet quenched-flow measurements demonstrate that ATP is rapidly hydrolyzed to give a products complex as in the wild-type. The nucleotide-free, open and closed states of a single tryptophan-containing construct, W501+, show distinct fluorescence spectra and susceptibilities to acrylamide quenching which indicate that W501 becomes internalized in the closed state. The open-closed transition does not require hydrolysis per se and can be induced by a nonhydrolyzable analogue. At 20° C, the equilibrium may favor the open state, but with ATP as substrate, the subsequent hydrolysis step pulls the equilibrium toward the closed state such that a tryptophan mutant containing only W501 yields an overall 80% enhancement. These studies allow solution-based assays to be rationalized with the crystal structures of the myosin motor domain and show that three different states can be distinguished at the interface of the relay and converter regions.

Tryptophan fluorescence has long been used to characterize myosin−nucleotide complexes in steady-state or transient kinetic studies (*1*, *2*). ATP binding and hydrolysis by rabbit skeletal muscle myosin subfragments is associated with a 10−20% enhancement in tryptophan emission intensity while, at the end of the reaction, the product ADP remains bound to give about a 5% enhancement. These studies, in conjunction with quenched-flow methods, showed that the predominant nucleotide state during the steady-state hydrolysis of ATP was a M**·ADP·Pi complex in a conformation distinct from the binary M*·ADP state formed after complete turnover of the ATP or by direct addition of ADP to myosin. Nonhydrolyzable (e.g., AMP·PNP)[1] or slowly hydrolyzable (e.g., ATPγS) nucleotides induced a fluorescence enhancement of amplitude between that observed for the M**·ADP·Pi and M*·ADP states (*1*, *2*).

Stopped-flow studies established that the nucleotide binding process was at least two-step with a fluorescence change occurring during a first order isomerization step, most likely of a myosin−nucleotide binary complex (*3*). The higher amplitude observed on ATP binding and hydrolysis to give M**·ADP·Pi indicated part of the fluorescence change coincided with the hydrolysis step itself (or an additional conformation change required for rapid hydrolysis to occur). These studies led to a commonly accepted mechanism for the ATPase as

$$\begin{array}{l} \mathrm{M + ATP} \overset{1}{\rightleftharpoons} \mathrm{M.ATP} \overset{2}{\rightleftharpoons} \mathrm{M^*.ATP} \overset{3}{\rightleftharpoons} \mathrm{M^{**}.ADP.Pi} \\ \qquad\qquad\qquad\qquad\qquad\qquad\qquad\qquad\qquad\qquad\qquad\qquad \updownarrow 4 \\ \mathrm{M + ADP} \overset{7}{\rightleftharpoons} \mathrm{M.ADP} \overset{6}{\rightleftharpoons} \mathrm{M^*.ADP + Pi} \overset{5}{\rightleftharpoons} \mathrm{M^*.ADP.Pi} \end{array} \quad (1)$$

where the asterisk (*) distinguishes conformational states and relates approximately to the level of tryptophan fluorescence enhancement (*3*, *4*). An exact assignment of fluorescence level of M*·ATP remained ambiguous because the enhancement by nonhydrolyzable ATP analogues is slightly greater than that of the corresponding M*·ADP state (*1*). With ATP itself, M*ATP remains a minor species, at least at 20° C, and the observed fluorescence is dominated by M**·ADP·Pi. These studies were performed before the high-resolution structure of the motor domain was solved by X-ray crystallography. Interest in this field has been rekindled by the need to relate nucleotide states observed in solution with those in crystals (*5*−*8*). In the latter case, nucleotide complexes (ADP·AlF_4, ADP·Vi) which are thought to mimic the M**·ADP·Pi state are associated with a movement of the switch II region toward the P_i analogue group. This triggers a movement in residues at the C terminus of the motor domain and a large swing in the angle of the regulatory domain. This so-called open-closed transition at the active site is

† This work was supported by BBSRC and the Wellcome Trust.

* To whom correspondence should be addressed. Phone: +44 (0)-116 252 3454. Fax: +44 (0)116 252 3369. E-mail: crb5@le.ac.uk.

[1] Abbreviations: AMP·PNP, adenosine 5′-($\beta\gamma$-imidotriphosphate); ATPγS, adenosine 5′-*O*-(3-thiotriphosphate); Dd, *Dictyostelium discoideum*; mant-, 2′(3′)-*O*-(*N*-methylanthraniloyl)-; Vi, vanadate; wt, wild-type.

10.1021/bi001125j CCC: $19.00 © 2000 American Chemical Society
Published on Web 12/02/2000

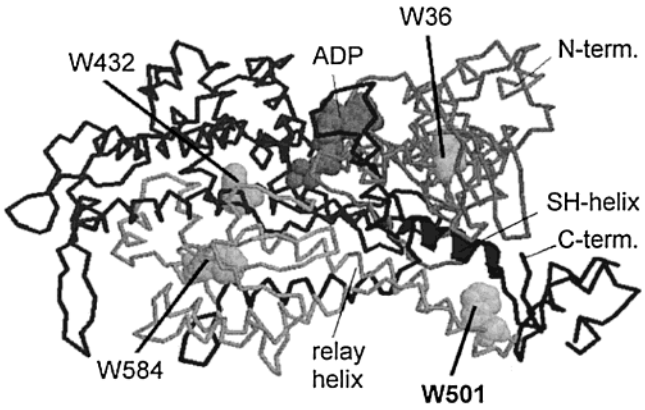

FIGURE 1: Backbone structure of the Dd myosin motor domain in the presence of ADP and Vi, as determined by Smith and Rayment (*6*), showing the location of the tryptophan residues.

considered a key step, since its reversal when the motor domain is bound to actin could represent a power stroke of the crossbridge cycle (*9*).

Although, in general, tryptophan fluorescence provides a signal for monitoring nucleotide interaction with myosin II, the amplitude of the enhancement varies between different species. In the case of the *Dictyostelium discoideum* (Dd) myosin II motor domain, ADP binding causes little change (<3%) in fluorescence and that induced by ATP has a smaller amplitude (5−10%) compared with rabbit skeletal myosin (*10*, *11*). Interestingly, Dd myosin II lacks tryptophan residues at the entrance to the nucleotide binding pocket corresponding to W113 and W131 in vertebrate skeletal myosin. However, it retains W501 (corresponding to W510 in rabbit), which has been proposed to sense the hydrolysis step (*12*, *13*). Although W501 is some 3.5 nm from the ATPase site, it is part of the relay region that faces the converter domain (Figure 1) and responds to the open-closed transition (*9*). The corresponding scheme for the Dd myosin motor domain can therefore be represented as

$$\begin{array}{ccccccc} \mathrm{M} + \mathrm{ATP} & \overset{1}{\rightleftharpoons} & \mathrm{M.ATP} & \overset{2}{\rightleftharpoons} & \mathrm{M\dagger.ATP} & \overset{3}{\rightleftharpoons} & \mathrm{M^*.ADP.Pi} \\ & & & & & & \downarrow 4 \\ \mathrm{M} + \mathrm{ADP} & \overset{7}{\rightleftharpoons} & \mathrm{M.ADP} & \overset{6}{\rightleftharpoons} & \mathrm{M\dagger.ADP + Pi} & \overset{5}{\rightleftharpoons} & \mathrm{M.ADP.Pi} \end{array} \quad (2)$$

The daggar (†) symbol is used to distinguish between isomeric states with similar fluorescence yields (these states actually show a small fluorescence quench as discussed below). Recently, Batra and Manstein (*14*) reported that mutation of W501 to tyrosine was accompanied by a loss of the ATP-induced fluorescence enhancement. We confirm this conclusion here using a related mutant W501F and examine a complementary construct in which all other tryptophans, except W501, have been changed to phenylalanine (W501+). The importance of the latter approach is 3-fold. (1) Loss of tryptophan signal in a W501− mutant enzyme could arise, in principle, from a change in rate-limiting step. The positive control, W501+, therefore, provides complementary evidence to support the response of W501 to the open-closed transition associated with hydrolysis. (2) Substitution of the three nonresponsive tryptophan residues (W36, W432, and W584) should result in an enhanced change in relative fluorescence of the remaining W501 on nucleotide addition and therefore better resolution of different conformational states. As a consequence, we have resolved additional states that were masked in the wild-type Dd motor domain. (3) The single tryptophan mutant, W501+, allows unambiguous assignment of the origin of spectroscopic signals. In the course of this study, we also made a tryptophan-less mutant, W−, which proved valuable for establishing conditions which minimized the contribution of tyrosine fluorescence to the emission signal.

Yengo and colleagues (*15*, *16*) have used single tryptophan mutants to investigate the actin-binding interface of smooth muscle myosin and have recently extended their studies to residue W512 equivalent to W501 in *Dictyostelium* (*17*). The comparisons that can be made at present suggest some differences in the response of this residue to nucleotide binding. Our data suggest that the enhancement of W501 tryptophan fluorescence does not correspond to the hydrolysis step per se, but the open-closed transition that precedes it. In addition, we show that nucleotide binding induces a quench in W501 fluorescence, prior to the enhancement arising from the open-closed transition. This reversal in signal intensity helps to remove an ambiguity in the definition of conformational states prior to hydrolysis.

MATERIALS AND METHODS

Protein Engineering. The Dd myosin II motor domain coding sequence was mutagenized to yield the following tryptophan variants. The M761 motor domain cDNA fragment (*18*) was subcloned into the pGEM-11Zf(+) vector (Promega), and the GeneEditor System (Promega) was used for the mutagenesis procedures. Three Trp mutants were constructed: W501−, W501+ (containing a single tryptophan), and W− (trp-less). W501− was created by mutagenising W501 to phenylalanine using the following primer: GAAGAATATCTTAAAGAGAAAATCAATTTC-ACTTTCATCGATTTTGGTC. In the W501+ construct, all tryptophans (W36F, W432F, and W584F) except W501 were changed to phenylalanine using the three primers: GAGATA-CATTTTCTATAATCCAGATCC, CGTCTTTTCCTCTTC-TTGGTCAAAAAGATCAACAATGTCC and GAGATTC-AAGATTTCTTAGAAAAGAACAAAGATCC. In W−, the remaining tryptophan in W501+ was changed using the first primer above to give a tryptophan-lacking construct. The mutagenized inserts were subcloned into the Dd pDXA-3H expression vector, developed by Manstein et al. (*19*), using the *Bam*HI sites. The expressed protein constructs contained a His_6 fusion at the C-terminus to allow a HisTag purification procedure (*20*). All constructs were verified by sequencing. Note that these constructs are based on the M761 motor domain (*18*) that differs from the M759 construct used in our previous studies (*11*), although their mechanisms appear comparable.

Dictyostelium Culture and Protein Preparation. Dd cells were grown HL5-5C media at 21 °C. Plasmids were transformed into AX2 cells (*14*) by electroporation (Gene Pulser II, Bio-Rad). Transformants were selected in the presence of 30 μg/mL of Geneticin G418 sulfate (Gibco-BRL), and the expression level of clones were screened by SDS−gel electrophoresis following a small scale HisTag affinity isolation in the presence of 7 M urea. Transformed Dd cells were grown in 2 L conical flasks containing 0.5 L of culture. The flasks were shaken at 115 rpm, and the cells were harvested at a density of 10^7/mL by centrifugation for

10 min at 3000 rpm. After washing the cells with PBS buffer, the HisTagged motor domains were purified as described (*20*). Protein concentrations were determined using Bradford Reagent (Sigma).

Fluorescence Measurements. Steady-state fluorescence time courses and spectra were measured with an SLM 48000 spectrofluorimeter using a 5 mm path-length cell. In critical measurements, tryptophan was excited at 295 nm with 0.5 nm slits to minimize photobleaching and reduce inner-filter effects arising from high nucleotide concentrations. Acrylamide quenching was used to determine the solvent exposure of W501. The fluorescence intensity change was measured at 335 nm (λ_{ex} = 295 nm) in the presence of varying concentration of acrylamide. The samples were mixed separately at different quencher concentrations and measured within 1 min to avoid contributions from a slow fluorescence change. The data were fit to the Stern−Volmer relationship: $F_0/F = (1 + K_{SV}[\text{acrylamide}])$, where F_0 and F are the fluorescence intensities in the absence and presence of acrylamide, respectively, and K_{SV} is the dynamic quenching constant. At high acrylamide concentrations, the slow fluorescence intensity change was more significant and the static component could not be determined.

Transient fluorescence measurements were carried out using Applied Photophysics SF17MV or SX18MV stopped-flow fluorimeters with WG320 or WG335 cutoff emission filters in combination with a UGII filter to block visible stray light. The dead time of these instruments is between 1.5 and 2 ms as determined by the reaction of 2,6 dichlorophenoindolphenol with ascorbate. The reduced stray light level of SX18MV holographic grating was crucial for characterizing small changes in fluorescence associated with some reactions and was generally used with a 320 nm filter alone. All reactions were studied in a buffer comprising 40 mM NaCl, 20 mM TES, and 1 mM $MgCl_2$ at pH 7.5 at 20° C and the reagent concentrations stated refer to the reaction chamber unless otherwise stated. Data were normally collected on a split or logarithmic timebase to ensure there were a significant number of data points for all phases of multistep reactions, but reactions are usually displayed on a linear time base. Pretrigger information was also collected in some cases to assess the efficiency of solution exchange in the mixing chamber. The ram profile of the SF18MV instrument was checked by monitoring its position using the in-built linear potentiometer. Rate constants were determined by least-squares fitting to an exponential function using the Applied Photophysics software or Kaleidagraph (Synergy Software, Pennsylvania) to yield a k_{obs} value. For the *i*th step in the mechanism (eq 1, etc.), the forward rate constant is defined as k_i, the reverse rate constant as k_{-i} and the equilibrium constant as K_i in the direction of the ATPase reaction.

ATPase Measurements. Nucleotides were purchased from Sigma Chemical Co. (Poole. U.K.) except mant-ATP, which was from Molecular Probes Inc. (Eugene, OR). The basal steady-state rate of the ATP hydrolysis was measured from A_{340} using a pyruvate kinase-lactate dehydrogenase linked assay (*21*). The assay was performed in 20 mM TES, 40 mM NaCl, and 2 mM $MgCl_2$ at pH 7.5 at 20° C in the presence of 1 mM ATP, 200 μM NADH, 400 μM PEP, 10 units/mL pyruvate kinase and 20 units/mL lactate dehydrogenase (P-0294, Sigma). The actin-activated Mg·ATPase activity was measured in the same conditions except at 5 mM TES and 5 mM KCl instead of NaCl and 17−76 μM F-actin. The F-actin was predialyzed against the assay buffer to avoid a change in ionic strength.

The progress of hydrolysis in the transient state was studied using a RQF-63 quenched-flow instrument (Hi-Tech Scientific, Salisbury, U.K.) or a custom-built, microquenched-flow apparatus that required only 60 μL of priming volume for each reagent (*22*). Two protocols were used. In one, the reaction was quenched with an equal volume of 0.2 M HCl and neutralized with 4 M NaOH solution, and then the protein was precipitated with an equal volume of absolute ethanol at −20 °C. The solution was diluted four times with 10 mM TES, pH 7.5, and loaded onto HR 5/2 column containing Source 15Q (Pharmacia) anion-exchange resin. A 0 to 0.5 M, NaCl salt gradient containing 10 mM TES, pH 7.5, was applied by the FPLC apparatus. The ratio of the (ADP):(ATP+ADP) peaks, monitored by A_{260}, was analyzed to determine the extent of hydrolysis. A perchloric acid quench was avoided as it interfered with the column separation. The second protocol required the use of γ-^{32}P-labeled ATP and was more precise at low fractional levels of hydrolysis. ^{32}P-labeled inorganic phosphate was assayed by phospho-molybdate formation and extraction into organic solvent. A total of 100 μL of reaction mixture was quenched with an equal volume of 1 mM sodium pyrophosphate and 6% (v/v) perchloric acid. The quenched solution was immediately frozen in dry ice/ethanol mixture for temporary storage. After melting the samples, 300 μL of 1% ammonium molybdate, 10% trichloracetic acid, 0.8 M sulfuric acid, and 2.3 mM sodium phosphate was added. The phospho-molybdate complex was extracted with 800 μL of isobutanol/ethyl acetate 1:1 (v/v) mixture. After centrifugation, an aliquot of organic phase was mixed with scintillation cocktail and activity was measured in a Beckman LS6000TA liquid scintillation counter. The specific radioactivity was determined from ^{32}P standards made by hydrolyzing the original γ-^{32}P-labeled ATP in 1 M HCl at 100 °C for 10 min.

ATPase rates were also estimated from the period of enhanced steady-state fluorescence when a limited (3−5 -fold) molar excess of nucleoside triphosphate was added to the construct. Mant-ATP was followed by direct excitation of mant fluorescence (356 nm) or via energy transfer from tryptophan (295 nm excitation). In cases where there was no significant tryptophan fluorescence signal (e.g., with ATPγS), turnover was followed by competition with mant-ADP. The added nucleoside triphosphate displaces the mant-ADP to give a reduction in fluorescence during the steady-state, but mant-ADP rebinds at the end of the turnover because the mant-ADP affinity for Dd myosin is 10 times than that of ADP (*11*). These assays provide a convenient way to check for turnover, but the derived rate constant may be a slight underestimate owing to nucleoside diphosphate inhibition.

RESULTS

The contribution of W501 to the overall fluorescence response of the Dd motor domain to nucleotide interaction was assessed by means of site-directed mutagenesis. Three constructs were made: W501− (i.e., W501F), W501+ (i.e., a W36F, W432F, and W584F triple mutant), and W− (i.e., a W36F, W432F, W501, and W584F quadruple mutant). All

Table 1: Steady-State ATPase Activities of Motor Domain Constructs[a]

	basal Mg·ATPase	actin-activated Mg·ATPase		
	k_{cat} (s^{-1}) (±SD for $n = 3$)	k_{cat} (s^{-1})	K_{app} (μM)	k_{cat}/K_{app} ($M^{-1}s^{-1}$)
wt	0.07 ± 0.01	2.2	59	0.37×10^5
W501+	0.06 ± 0.01	2.5	64	0.39×10^5
W501−	0.21 ± 0.02	0.82	22	0.37×10^5
W−	0.21 ± 0.05	0.75	25	0.30×10^5

[a] The actin activated Mg^{2+}-ATPase activity was measured in the presence of 17−76 μM actin in 5 mM TES, 5 mM KCl at 20 °C. Values for k_{cat} and K_{app} were calculated by fitting the data to Michaelis−Menten equation.

these constructs showed good expression and yielded 1−2 mg of protein/g cells and were stable stored on ice for at least 2 weeks. Furthermore, they all showed Mg·ATPase activity, although it was noteworthy that the basal steady-state rates of the W501− and W− constructs were three times those of the wt and W501+ constructs, while their actin-activated ATPases were about 3-fold less (Table 1). Further work is required to evaluate the significance of the decrease in the apparent K_m for actin of mutant constructs lacking W501.

Figure 2a shows the emission spectra for these constructs when excited at 295 nm and the effect of ATP addition. In the absence of nucleotide, W501 is the most red-shifted emitter. To a first approximation, the tryptophan signals of W501− and W501+ summed to give the wild-type fluorescence emission, and W501 made about a 25% contribution to the wild-type fluorescence. At 295 nm excitation, the trp-less W− construct showed little emission, but displayed the characteristic tyrosine signal when excited at 280 nm (Figure 2a, inset).

On addition of ATP, the wild-type showed a 13% enhancement, W501− a 7% quench, W501+ an 80% enhancement in tryptophan fluorescence (Figure 2a) while W− showed no change in tyrosine fluorescence (not shown). These results confirm W501 is uniquely enhanced on interaction with ATP. There was a clear 7 nm blue shift in W501+ mutant fluorescence emission on ATP addition that was not apparent in the wild-type. This is because the unresponsive tryptophan residues in the wild-type (W36F, W432F, and W584F) are already blue-shifted relative to W501, and thus mask the underlying shift of W501 fluorescence in the presence of ATP. Interestingly, ADP binding to the W501+ construct gave a 17% quench in fluorescence (Figure 2b), which was titrated to yield an equilibrium constant of about 5 μM. The quench was associated with a 4 nm blue shift, indicating there are at least two distinct nucleotide-bound conformational states rather than the nucleotide-free state lying between the +ATP and +ADP states. Reexamination of the wild-type construct also revealed a small fluorescence quench (7.5%) on ADP addition, indicating that the quench in W501+ was not a consequence of mutagenesis. To observe maximal fluorescence changes, it was important to use narrow (0.5 nm) excitation slit widths so as to minimize background signal from light scattering and tyrosine fluorescence. In previous studies, the reported change of <3% in the wt motor domain on addition of ADP was determined with wider slit widths and was not sufficient to characterize binding, particularly with the SF17MV

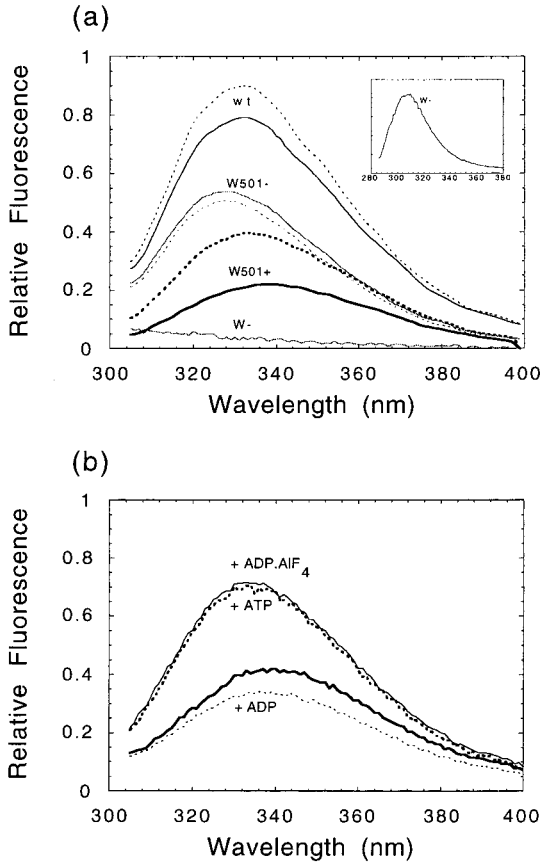

FIGURE 2: (a) Uncorrected fluorescence emission spectra of *Dictyostelium* constructs in the absence (—) and presence (···) of ATP. Spectra of wild type, W501+, W501−, and W− myosin motor domain constructs (6 μM) in the absence or presence of 200 μM ATP were recorded at 20 °C in 20 mM TES, 40 mM NaCl, and 2 mM $MgCl_2$ at pH 7.5. Tryptophan fluorescence was excited at 295 nm (excitation slit width = 0.5 nm, emission slit width = 4 nm). The inset shows the tyrosine emission spectrum of the W− myosin construct on excitation at 280 nm. (b) Uncorrected fluorescence emission spectra of W501+ construct in the absence (—) and presence of 50 μM ATP (- - -) or ADP (- - -). The AlF_4 complex (—) was made by addition of 55 μM $AlCl_3$ and 3 mM NaF to the W501+. ADP complex and the spectrum measured after 2 h.

stopped-flow apparatus which has a higher stray light level (*11*).

Phosphate analogues have been exploited in X-ray crystallography to generate long-lived intermediates that mimic the steady-state products complex (*5*−*9*). Addition of AlF_4- to the M·ADP state caused a slow rise in fluorescence (k_{obs} = 7×10^{-4} s^{-1} at 55 μM AlF_4-) to give a spectrum that closely matched that of ATP in the steady-state (Figure 2b). BeF_3-induced a similar enhancement to that by AlF_4- at 20 °C, but at 4 °C the signal was significantly smaller. The corresponding Vi complex was not studied because this phosphate analogue absorbs strongly in the ultraviolet and results in a significant inner filter effect at the excitation wavelength of tryptophan.

The ATP-induced change in tryptophan fluorescence of these constructs was studied under single turnover conditions in a stopped-flow apparatus (Figure 3). As expected, W501+ showed an enhancement phase due to ATP binding and hydrolysis, followed by a slow recovery associated with product release. The observed amplitude of enhancement (about 23%) was less than the spectral measurements in

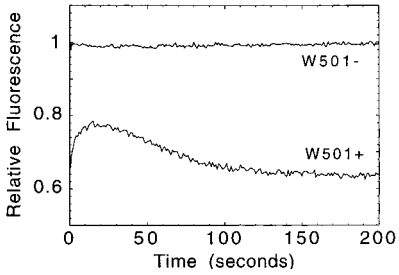

FIGURE 3: Single turnover of ATP by W501+ and W501− constructs. Protein (2 μM) was mixed with 1.8 μM ATP in the stopped-flow apparatus and tryptophan fluorescence was followed on excitation at 295 nm and the emission selected using a WG335 filter. The data were corrected using a buffer blank to define zero fluorescence and the W501− signal was normalized to 1.

Figure 2 for at least three reasons. At the concentrations used, the binding phase was less than an order of magnitude faster than the turnover phase, so the peak fluorescence is reduced in Figure 3. Furthermore, the wider excitation slits ($\geq$4 nm) and the use of cutoff filters in the stopped-flow measurements gives a higher background contribution from scattering and tyrosine fluorescence. Figure 3 was recorded using the SF17MV instrument that had a higher stray light level than the SF18MV used in later experiments. Nevertheless, the observed change for W501+ in Figure 3 is significantly larger than that of the wild-type M761 or M759 construct (10%) in the same instrument (*11*). On the other hand, no significant change in tryptophan fluorescence (<2% quench) was seen on interaction of ATP with the W501− construct (Figure 3). While this result is in accord with the conclusion that W501 is the only residue to contribute to the enhancement in fluorescence (*14*), it is possible that the open-closed transition or the hydrolysis step has been slowed to a sufficient degree that it becomes rate-limiting in the W501− construct. Hence an M·ATP-like state could become predominant in the steady-state. This possibility was ruled out by a quenched-flow experiment in which 10 μM ATP was mixed with 12 μM W501− construct and the nucleotide products were analyzed by anion-exchange chromatography. After 2 s, when the binding phase is likely to be nearly complete but product release has barely started, 65% of the ATP had been hydrolyzed. A second slower phase of ATP hydrolysis was observed which could be attributed to the reversible hydrolysis equilibrium on the enzyme (*3*, *11*), or possibly, the presence of inactive enzyme leading to a slight excess of [ATP] over [W501− construct]. From the relative amplitudes of the fast and slow phases, we estimate the hydrolysis equilibrium constant (eq 2; K_3) to be $\geq$2 for W501−, and hence an M*·ADP·Pi-like state (Eqn. 2) should predominate in the steady-state, but it remains optically silent.

Further studies focused on the W501+ construct that gave a large fluorescence enhancement with ATP. When a limited excess of ATP was added to the W501+ construct, the period of enhanced fluorescence indicated a turnover rate of 0.045 s^{-1} (Figure 4a), in line with the steady-state k_{cat} value (Table 1). On the other hand, addition of ATPγS induced $\leq$4% enhancement in the steady-state fluorescence. Nevertheless, ATPγS is a substrate for the W501+ construct as demonstrated by a competitive turnover assay with mant-ADP (Figure 4b). Previous studies have shown that ATPγS is slowly hydrolyzed by vertebrate myosin, but the products are released relatively quickly, so that an M*·ATP complex,

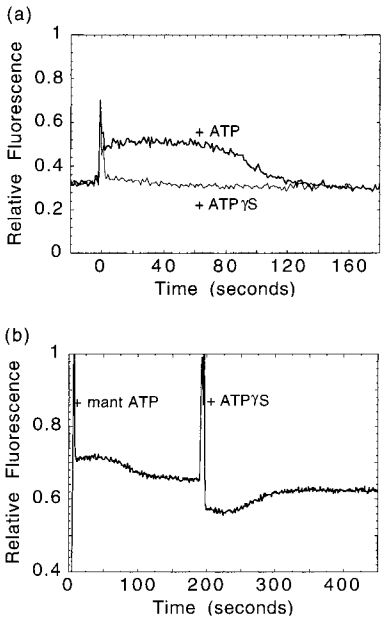

FIGURE 4: (a) Turnover of ATP and ATPγS by W501+ construct monitored by tryptophan fluorescence enhancement. W501+ (2 μM) W501+ motor domain was mixed with 8 μM ATP (bold line) or ATPγS. Fluorescence was excited at 295 nm (1 nm slit) and emission was observed at 335 nm (4 nm slit). The period of enhanced fluorescence indicates a turnover rate of ATP of 0.045 s^{-1}. (b) Turnover of mant-ATP and ATPγS by the W501+ construct monitored by mant fluorescence. W501+ (2 μM) motor domain was mixed with 8 μM mant-ATP. After hydrolysis to mant-ADP, 8 μM of ATPγS was added. The reaction was followed by excitation at 356 nm (2 nm slit) and emission at 450 nm (4 nm slit). The periods of steady-state fluorescence indicate that mant-ATP and ATPγS are turned over with rate constants of about 0.047 and 0.053 s^{-1} respectively. Buffer conditions were as in Figure 2.

rather than an M**·ADP·Pi complex (eq 1), dominates the steady-state intermediates (*2*, *3*). The above experiments are self-consistent and provide direct evidence that the emission from W501 is uniquely enhanced during the hydrolysis step (or the preceding open-closed transition that limits hydrolysis). The studies described below revealed additional features of the mechanism which helped to pinpoint the step associated with the fluorescence enhancement of W501.

The observed quench in W501+ tryptophan fluorescence on addition of ADP (Figure 2b) indicates that W501 also responds to the binding of nucleotide in a step that is distinct from the open-closed transition or hydrolysis step. To explore this further, the kinetics of binding of different nucleotides were examined in a stopped-flow apparatus. Figure 5a shows the fluorescence change on the millisecond time scale when ATP, ADP, and ATPγS interact with the W501+ construct. ATP shows a 30% enhancement, ADP shows a 10% quench, while ATPγS shows a small quench followed by a small enhancement, then a further quench on the seconds time scale.

The ADP profile is the simplest to interpret as it is essentially a single phase. The observed rate constant is linearly dependent on [ADP] and revealed an apparent second-order association rate constant of 1.4×10^6 M^{-1} s^{-1}. (Figure 6a), although at concentrations of >100 μM ADP, there is an indication of saturation with a first-order rate constant of >400 s^{-1}. This behavior is similar to that of rabbit skeletal S1 (*3*, *4*), although in the latter case the process is associated with a fluorescence enhancement of other tryp-

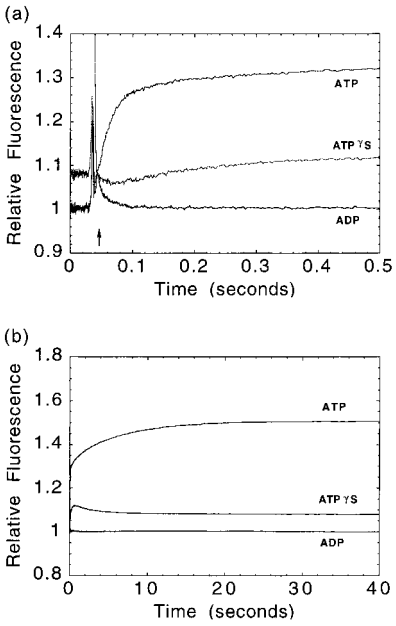

FIGURE 5: Stopped flow records of 1.1 μM W501+ on mixing with 50 μM ATP, ADP, or ATPγS. Buffer conditions were as in Figure 2. Panel b shows the same records as in panel a, but on a longer time base. The arrow indicates the time of stopping the flow. Note that the pretrigger signals in panel a correspond to the end point of the preceding push of the reactions in panel b.

tophan residues which presumably swamp any quench of the equivalent W510. It is likely that ADP binding is at least two step in Dd myosin, with a fluorescence quench in W501 associated with an isomerization indicated by the daggar (†).

$$\mathrm{M} + \mathrm{ADP} \underset{7}{\rightleftharpoons} \mathrm{M.ADP} \underset{6}{\rightleftharpoons} \mathrm{M\dagger.ADP} \qquad (3)$$

The rate constant for dissociation of ADP from the M†·ADP state was determined to be 7.9 s^{-1} on displacement by excess ATP (Figure 6b). This value is consistent with the intercept value of k_{obs} versus [ADP] for the association reaction (5.6 s^{-1}, Figure 6a) and yields a dissociation equilibrium constant for the M†·ADP complex of 5.6 μM. It is also comparable to that estimated by titration (see above) and close to that for the wild-type M759 motor domain estimated from competition with mant-ADP binding (*11*).

It is of interest to know whether there is a corresponding quenched M†·ATP state, prior to the large enhancement associated with the open-closed transition or hydrolysis. At 20° C, there is a noticeable lag phase in the enhancement induced by ATP on long time-base records (Figure 5a), but it is more difficult to assess whether there is a genuine quench in signal immediately after stopping the drive syringes. A lag would be expected simply on the basis of a spectroscopically silent isomerization (eq 2, step 2) prior to hydrolysis (step 3) which is associated with the fluorescence enhancement (see below). The detailed interpretation of the ATP interaction is best considered after discussion of other analogues.

In support of the conclusion that W501 generally responds to nucleotide binding with an initial decrease in emission intensity, a clear quench was seen on interaction with ATPγS at 20° C (Figure 5a). The subsequent enhancement indicates that the W501+ construct undergoes an open-closed transition and/or hydrolysis, but the limited amplitude argues that

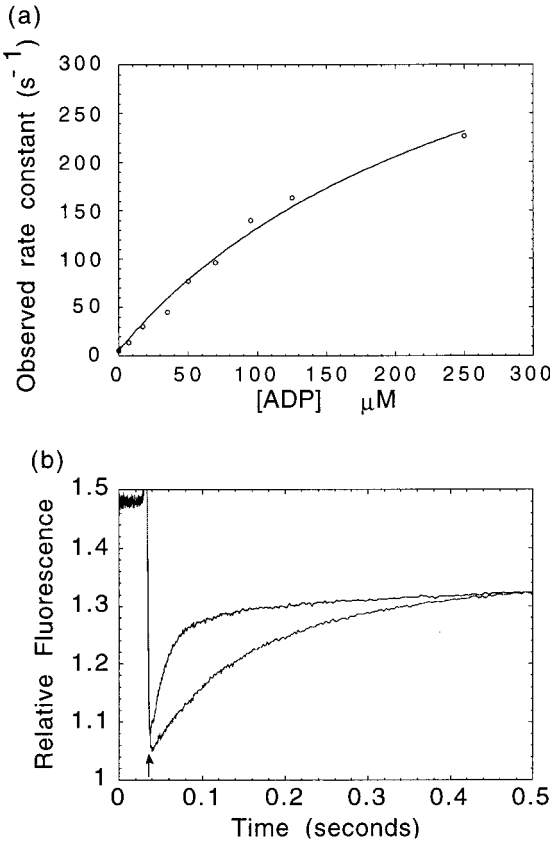

FIGURE 6: ADP association with and dissociation from W501+ construct followed by tryptophan fluorescence. (a) A plot of the observed pseudo-first-order rate constant for the fluorescence quench (see Figure 5a) against ADP concentration to yield an apparent second-order ADP association rate constant of 1.4×10^6 M^{-1} s^{-1} and a saturation with a first-order rate constant of >400 s^{-1}. (b) The rate constant for ADP dissociation determined displacement by excess ATP. The faster record was obtained on mixing 500 μM ATP with 1.1 μM W501+, while the slower record contained 50 μM ADP premixed with the 1.1 μM W501+ (reaction chamber concentrations), to yield an ADP dissociation rate constant of 7.9 s^{-1}. Buffer conditions were as in Figure 2.

the M†·ATPγS state remains a predominant species. The final fluorescence decrease on the seconds time scale (Figure 5b) could arise as M†·ADP builds up to a low steady-state level. The final steady-state fluorescence is close to that for the nucleotide-free state of Dd W501+, in agreement with the low time resolution record in Figure 4b.

Although ATPγS proved a useful analogue to reveal the initial quench in W501 fluorescence on binding, the interpretation of the subsequent rise in emission is ambiguous because slow hydrolysis could result in a small but finite level of an M*·ADP·Pi-like state (eq 2). The interaction with the nonhydrolyzable analogue, AMP·PNP with the W501+ construct was therefore examined. At 20 °C, this gave a similar profile to that for ATPγS over the first second, but with an initial lag rather than a quench in fluorescence (Figure 7). The temperature dependence of the reaction was particularly revealing. At 26 °C, the lag was very small, but the rise in fluorescence was marked (10% enhancement). On the other hand, at 9 °C, a 10% quench in fluorescence was observed with no recovery phase. Preincubation of the AMP·PNP preparation with catalytic amounts of W501+ to remove any potential ATP contamination did not alter the observed changes. These results demonstrate that the enhancement in

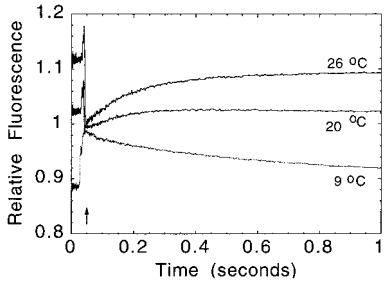

FIGURE 7: Stopped-flow records of the reaction of 1.5 μM W501+ construct with 60 μM AMP·PNP at different temperatures. For ease of comparison, the fluorescence values corresponding to the nucleotide-free W501+, present immediately after stopping the flow (indicated by the arrow), were set to a value of 1 by shifting the original records by −0.53, −0.18, and − 0.06 for the 9, 20, and 26 °C records, respectively. These differences largely reflect the temperature dependence of intrinsic tryptophan emission process. Buffer conditions were as in Figure 2. Note that the pretrigger signal of each trace can be identified from its value compared with the endpoint reached after 1 s.

W501 does not require the hydrolysis reaction per se and therefore implies that the rise in fluorescence is associated with the preceding open-closed transition. However, the equilibrium constant for the latter transition lies toward the open state, particularly at low temperatures, and hydrolysis is required to pull the reaction toward the closed state (cf. *9*).

$$\mathrm{M + AMP.PNP} \overset{1}{\rightleftharpoons} \mathrm{M.AMP.PNP} \overset{2}{\rightleftharpoons} \underset{\text{Open}}{\mathrm{M^{\dagger}.AMP.PNP}} \overset{3a}{\rightleftharpoons} \underset{\text{Closed}}{\mathrm{M^{*}.AMP.PNP}} \quad (4)$$

AMP·PNP and ATPγS, therefore, only give limited fluorescence enhancements compared to that of ATP. The open-closed transition is very temperature dependent. Assuming that ADP gives predominately the open state and ATP predominately the closed state in the steady-state, and that the open and closed states have a specific fluorescence intensity independent of nucleotide, we estimate from the end-point fluorescence value that the open-closed transition (step 3a) has an equilibrium constant of ∼0.04 at 9° C, ∼0.2 at 20 °C, and ∼0.5 at 26 °C for AMP·PNP interaction. These values indicate that the open-closed transition is a very endothermic reaction (see Discussion). At 26° C, a net enhancement in fluorescence is observed (Figure 7) even though $[M^{\dagger}\cdot AMP\cdot PNP]_{open} \approx [M^{*}\cdot AMP\cdot PNP]_{closed}$ because the latter has a higher intrinsic enhancement (*) compared with the intrinsic quench (†) of the former. The qualitative conclusions that the transition(s) associated with the fluorescence enhancement is readily reversible and very temperature dependent hold even if the assumptions about the exact level of fluorescence of the open and closed states are inaccurate. Displacement of AMP·PNP from its bound complex(es) by excess ATP has an observed rate constant of 0.017 s^{-1} at 20° C. This implies that k_{-2} (eq 4) has a rate constant of approximately 0.02 s^{-1}, because the equilibrium of step 3 has a minor effect on the back rate at this temperature [$k_{-2} = k_{obs}\ (1 + K_3) = 1.2 \times 0.017\ s^{-1}$]. The first step, by analogy with the binding other nucleotides, represents a weak and rapidly reversible step (i.e. $k_{-1} > k_{-2}$).

In light of these results, the interaction of ATP with W501+ can be considered further. Figure 8a shows representative traces of enhancement in W501 fluorescence induced by different concentrations of ATP at 20 °C. The large enhancement in W501 fluorescence indicates that the hydrolysis of ATP pulls the open-closed transition to the right. The lag associated M*·ADP·Pi formation makes minor contribution to the signal and the first phase of enhancement can be reasonably fit to a single exponential over >80% of its profile. The error in fitting comes mainly from the deviation caused by a slower phase in enhancement (see below). At low [ATP], the resultant rate constant was linearly dependent on concentration, but the process saturated at a maximum of 30 s^{-1}, comparable to that for the wild-type Dd motor domain (*11*, *18*). However, it should be noted that this value has proven rather variable between different preparations and different constructs [but the value is invariably smaller than the maximum rate of acto-motor domain dissociation which is 150 to 400 s^{-1} (*11*, *18*)]. The limiting rate constant may be assigned to that of the open-closed transition coupled to the hydrolysis reaction ($k_3 + k_{-3}$ in eq 2). The profile of k_{obs} against [ATP] was not hyperbolic (Figure 8b). This is to be expected because the fluorescence enhancement occurs after the binding step that itself involves an essentially irreversible isomerization ($k_{-2} \ll k_3$ by analogy with skeletal myosin). Thus, the [ATP] concentration that gives an apparent k_{obs} of 50% the maximum (45 μM) corresponds to the condition when $K_1k_2[ATP] = k_3 + k_{-3}$ and results in a profile with a lag phase. Force fitting a single exponential to this profile gives a rate constant with a value close to $(k_3 + k_{-3})/2$. From the linear dependence of k_{obs} on ATP, at low concentrations, the value of K_1k_2 is estimated to be $0.66 \times 10^6\ M^{-1}\ s^{-1}$.

In principle, the raw data could be fitted globally using a two-step model for ATP binding and hydrolysis. However, it is likely that the M†·ATP state is not optically silent, but contributes a small quench in fluorescence (approximately 10% by analogy with ADP) that would introduce another parameter into the equation. Furthermore, the results with AMP·PNP suggest that the open-closed transition will occur to a limited extent in the absence of a subsequent hydrolysis reaction. If such a process occurs with ATP as substrate, then there should also be a small burst phase in fluorescence enhancement prior to the main enhancement phase that is coincident with the hydrolysis reaction. This would tend to counteract any initial quench (cf. the record for AMP·PNP binding at 20 °C, Figure 7). Modeling such a scheme shows that if a 10% fluorescence quench is assigned to the M†·ATP state, the observed quench is <5% as a result of "truncation" by the subsequent enhancement phase. Furthermore, at high [ATP], when the first two steps would be best resolved from the hydrolysis reaction, >25% of the signal change would be lost in the dead time of the instrument (cf. the ADP records at >100 μM). Nevertheless, such modeling indicates that at least part of the phase of decreasing fluorescence should be observable in the SF18MV stopped-flow instrument if the M†·ATP state has a 10% quench. The measurement has to be executed with care, because during the flow period, the solution from the previous shot will generally be in the high fluorescent M*·ADP·Pi state which must be expelled and the signal detector response must be sufficiently fast to avoid it contributing to an artifactual decrease in signal at the time of stopping. Figure 8c shows two such experiments on mixing 50 μM ATP with 1.1 μM W501+ in which the time between pushes was varied. The delivery volume was set at 2×70 μL i.e., over three times

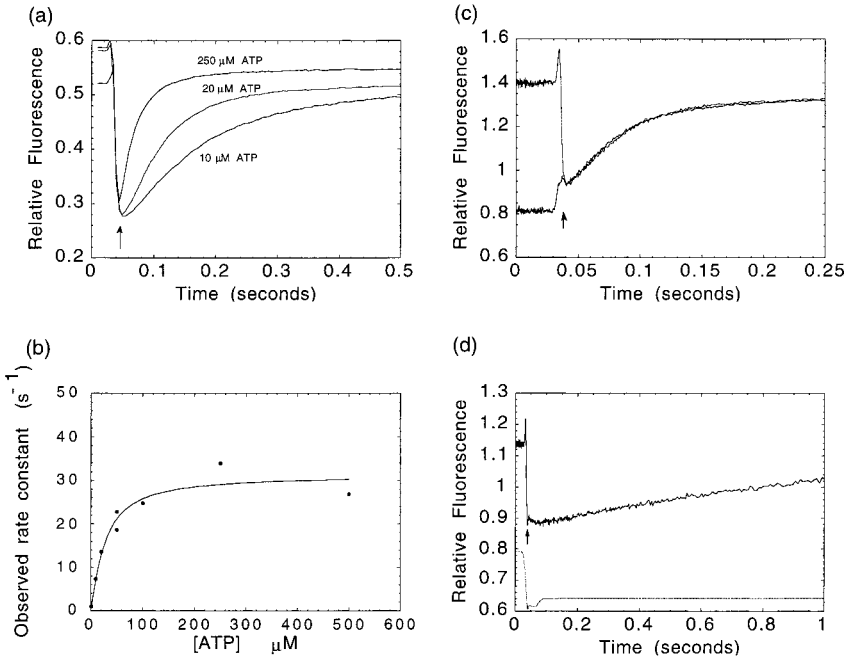

FIGURE 8: (a) Stopped-flow records of the reaction of 1.1 μM W501+ construct with 10, 20, and 250 μM ATP. The arrow indicates the flow stop. (b) A plot of the pseudo first-order rate constant for the ATP reaction as a function of [ATP]. Records, such as those in panel a, fitted to a single exponential over 80% of their profile (see text) and yielded a maximum rate constant of 30 s^{-1} at saturating [ATP]. (c) Reaction of 50 μM ATP with 1.1 μM W501+ at 20 °C in which the waiting time between pushes was varied. The top trace starts from the previous M*·ADP·Pi state while the bottom one starts from the M†·ADP state. The signal of 1.0 ± 0.05 was set using the same W501+ concentration after mixing with buffer. (d) The same reaction as panel c but at 3 °C. The bottom trace is a linear potentiometer record that monitors the drive syringe position. Note that the fluorescence signal decrease after the drive has become stationary. The subsequent rise in the potentiometer trace corresponds to the pressure release from the drive ram, but is not associated with any significant movement of the solution in the reaction chamber as judged by the fluorescence record.

the observation cell volume (40 μL). In one record, sufficient time was allowed for the ATP to be turned over by the W501+ construct in the reaction chamber so that the fluorescence fell to that of the M†·ADP state and hence the washout profile reverses in direction. Both traces however show about a 2% fluorescence decrease immediately after stopping the flow which would appear to reflect a genuine quench rather than flow artifact, although slight recoil of the syringes is difficult to rule out completely. The presence of a quench phase was confirmed by carrying a similar experiment at 3° C, where the initial decrease in fluorescence (2% amplitude) occurred over 30 ms, well resolved from any flow or mixing artifacts (Figure 8d). These data support the proposal that an early intermediate in the ATP turnover pathway is a binary complex, (M†·ATP) that has a quenched fluorescence relative to the nucleotide-free state. However, the records are not sufficiently resolved from the dead-time, and the subsequent steps associated with an enhancement of fluorescence to establish whether M†·ATP and M†·ADP have identical fluorescence yields. This ambiguity also prevents determination of a unique value for k_2 for ATP, although values around 400 s^{-1}, by analogy with ADP, are consistent with these results. The data obtained at 3 °C, where signals would be expected to be better resolved, suggest M†·ATP may be less quenched than M†·ADP, but a full characterization of all intermediates is required at each temperature because temperature affects both the distribution of states and intrinsic fluorescence properties of tryptophan emission.

At high ATP concentrations, a second slow phase of enhancement (k_{obs} = 0.17 s^{-1}) was revealed which was concentration independent (Figure 5b). The amplitude of this phase varied from 10 to 30% of the overall change with different preparations. The significance of this phase is unclear, but it appears to represent a subsequent isomerization of the M*·ADP·Pi complex. Other interpretations of this phase were considered. Such a first-order reaction could arise if a fraction of the active sites were occupied with a tight-binding inhibitor acquired during protein preparation. Extensive dialysis did not remove the slow phase. More revealing were the profiles observed on mant-ATP binding (Figure 9). When the mant fluorophore was excited directly (356 nm), only a single enhancement phase was observed, with a slight (<5%) decrease in signal on the seconds time scale (possibly attributed to small contribution from M·mant-ADP in the steady state). On the other hand, the same

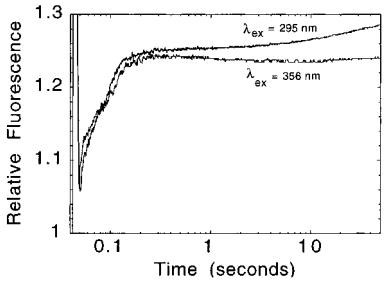

FIGURE 9: Stopped flow records of the reaction of 1.1 μM W501+ construct with 50 μM mant-ATP. The mant fluorophore was excited directly at 356 nm or via energy transfer from W501 at 295 nm. Buffer conditions were as in Figure 2. The reactions are displayed on a logarithmic time base following the trigger signal (first time point after trigger was at 0.05 s). The amplitudes of the reactions were normalized to the beginning and end of the fast phase to demonstrate that there is a further slow increase in mant fluorescence emission only when monitored via excitation of W501.

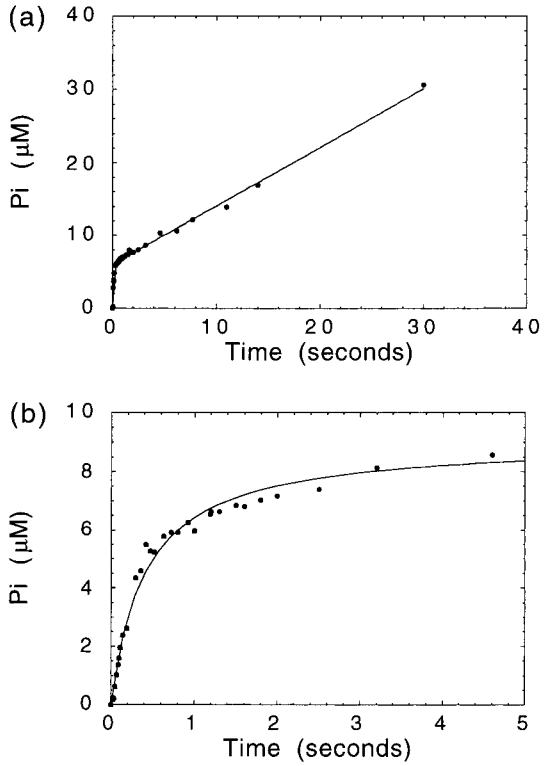

FIGURE 10: Hydrolysis of ATP by the W501+ construct followed by quenched-flow. (a) The reaction of 100 μM γ-[^{32}P]-ATP with 15 μM W501+ construct quenched with perchloric acid. The fitted line corresponds to a burst of Pi production at 7.5 s^{-1}, followed by a steady-state phase at 0.066 s^{-1}. The W501+ preparation was different to that used in Figure 8 and revealed a fluorescence enhancement of 12 s^{-1} when mixed with 100 μM ATP. (b) A single turnover of nominal 10 μM γ-[^{32}P]-ATP by 15 μM W501+ construct. The fitted line is for the second-order binding equation $[Pi]_o - [[Pi]_o/([Pi]_o kt + 1)]$, and yields an apparent association rate constant $k = 0.27$ μM^{-1} s^{-1} and final amplitude of 9 μM Pi. A biphasic exponential fit to the same data yielded rate constants of 3.3 s^{-1} (5.5 μM) and 0.32 s^{-1} (0.32 μM).

reaction mixture monitored via energy transfer from W501 by excitation at 295 nm, yielded a fast phase which superimposed (when normalized) that for direct excitation, followed by a further increase (10%) on the seconds time scale. This argues that W501 is responding to a slow isomerization of a bound nucleotide state, rather than the W501+ construct having different conformational states prior to nucleotide binding (in which case they would be detected by mant-ATP binding regardless of the mode of excitation). This experiment also rules out that the slow phase on nucleoside triphosphate binding arises from displacement of a prebound ligand, such as ADP.

To explore the relation between W501+ tryptophan fluorescence and the hydrolysis reaction further, quenched flow studies were carried out under multiple and single turnover conditions. When ATP was in excess of the active site concentration, a burst of P_i production was observed at 7.5 s^{-1}, followed by a steady-state phase with $k_{cat} = 0.066$ s^{-1} (Figure 10a). A control stopped-flow experiment using the same protein preparation yielded a rate constant for the fluorescence enhancement of 12 s^{-1} at 100 μM ATP. Taken at face value, these data indicate that the fluorescence enhancement has a component that precedes the hydrolysis reaction. However, the small difference between the rate constants for fluorescence enhancement and phosphate release steps are probably within the error of the measurement, particularly as this reaction has an extreme dependence on temperature. Also when the quenched-flow apparatus is used with small (50 μL) volumes, there may be a small timing error introduced during the acceleration and braking phases. The burst amplitude, based on a protein concentration determined using Bradford reagent, was 0.4 μM P_i/μM W501+, indicating reversibility of the hydrolysis step and/or some inactive protein.

Table 2: Collisional Quenching Constants for the W501+ Construct[a]

nucleotide	Stern−Volmer constant K_{SV} (M^{-1})
none	4.18 ± 0.03
ATP	2.72 ± 0.02
ADP	3.10 ± 0.03

[a] W501+ (2.5 μM) was titrated with up to 0.6 M acrylamide in the absence and presence of 0.4 mM ATP or ADP at 20 °C.

When the protein was in nominal excess (Figure 10b), the production of Pi appeared biphasic with rate constants of 3.6 s^{-1} (amplitude = 5.5 μM) and 0.32 s^{-1} (amplitude = 0.32 μM). However, if the protein was not fully active, binding might occur under second-order conditions which has a longer "tail" than a pseudo-first-order reaction. The reaction could be fitted to the second-order equation almost as well as a biphasic exponential and yielded an apparent second-order binding rate constant was 0.27 μM^{-1} s^{-1}, without the need for a second phase. Consequently, it is difficult to establish the significance of the apparent slow phase from these data. Nevertheless, after allowing for the limited release of P_i by turnover, the hydrolysis reaction is at least 72% complete after 5 s and suggests $K_3 \geq 2$. The quench flow studies confirm that there is a burst of Pi production in the W501+ construct, with a rate that is comparable to that of the fluorescence enhancement, and that the hydrolysis equilibrium favors the M*·ADP·Pi state (eq 2), particularly as it probably occurs in conjunction with an unfavorable open-closed transition (see Discussion).

A single tryptophan-containing protein is valuable for detailed spectroscopic characterization because its properties can be assigned to a specific location in the protein. Acrylamide-quenching experiments were carried out to assess the exposure of W501 to solvent (*23*). The data suggest that W501 becomes more inaccessible in the M*·ADP·Pi state, but the differences in the Stern−Volmer coefficients were small (Table 2) and the titrations had to be carried out quickly so that the signals were not dominated by time-dependent changes.

DISCUSSION

The tryptophan residue W501 is located in the relay loop of the motor 50K domain (*5*−*8*) that faces the SH-helix of the converter region of myosin (Figure 1) and changes conformation during the ATPase cycle. Batra and Manstein (*14*) demonstrated that a mutant Dd myosin motor domain lacking W501 showed no tryptophan enhancement on addition of ATP. We confirmed this result using a W501F construct, but found that this preparation has a slightly higher basal ATPase rate. In principle, a loss of fluorescence enhancement could arise if hydrolysis were to become a rate-limiting step in the cycle (e.g., as with ATPγS as substrate

with wild-type). Nevertheless, Batra and Manstein (*14*) showed that the W501Y mutant retained reasonable actin-activation and suggested that the ATPase mechanism was almost unchanged. Here we demonstrate directly by quenched flow measurements that the W501− mutant displays a products burst, and thus the predominant species on ATP addition is equivalent to the M*·ADP·Pi complex (eq 2) but it is optically silent owing to the lacking tryptophan.

The slightly higher basal ATPase rate of mutations of the type W501F is a frequent characteristic feature of mutations in the converter domain itself (e.g., G691A; ref *24*) and of reactive SH-modified myosins (*25*). Instability in this region leads to a less stable M*·ADP·Pi complex and more ready loss of P_i. Batra and Manstein (*14*) did not detect any change in the basal rate with the W501Y mutation, although this construct also differed in having a two α-actinin repeats at the C-terminus that may help to stabilize the neck region. On the other hand, R. B. Patterson (personal communication) has found a number of temperature-sensitive W501 mutations in the Dd myosin gene which show aberrant phenotypes at the nonpermissive temperatures (e.g., W501L is cold sensitive). Nevertheless, even the trp-less mutant retains an essentially wild-type mechanism allowing tryptophan residues to be added almost at will as site-selective probes throughout the motor domain (cf. refs *15* and *16*).

The unique involvement of W501 in response to ATP interaction was confirmed using the W501+ construct that displays a large relative tryptophan enhancement, compared with the wild-type, because the signal of the latter includes a contribution from three additional unresponsive tryptophan residues. The single tryptophan construct also revealed a distinct 7 nm blue shift which was not resolved in the wild-type multitryptophan emission spectrum. This suggests W501 has a less polar environment in the presence of ATP and agrees with the observation that its side chain becomes protected from collisional quenchers (Table 2; refs *12* and *13*). We also show that W501 responds to an earlier step in the nucleotide binding mechanism that results in a 17% quench in fluorescence and a blue shift. This step appears to correspond to one in rabbit skeletal myosin that is associated with an enhancement in fluorescence. Given that the wild-type Dd myosin lacks this enhancement (and indeed shows a small quench), it is likely that the residues involved in the skeletal myosin enhancement on binding nucleotide are W113 and/or W131 that are located near the active site.

During the hydrolysis of bound ATP by myosin, X-ray crystal structures suggest that the switch 2 helix moves toward the γ-phosphate allowing the carbonyl group of Dd G457 to hydrogen bond with it (*5*, *6*). This movement from the open to closed state of the active site is accompanied by rotation of the converter region by about 70° and concomitant swing of the putative lever arm (*7*). Geeves and Holmes (*9*) argue that it is only then that hydrolysis can proceed, but it does so rapidly and reversibly. Accordingly, the fluorescence change of W501 effectively occurs with a rate constant that limits the observed hydrolysis time course, although it is actually monitoring the preceding open-closed transition. This idea is supported by Sutoh and colleagues' (*26*, *27*) findings that some Dd mutants (e.g., E459A) become trapped in a tightly bound ATP state which exhibits an enhanced tryptophan fluorescence and a lever arm swing as monitored by fluorescence resonance energy transfer. We provide direct evidence that the open-closed transition and hydrolysis are distinct steps in that AMP·PNP at temperatures of >20 °C can induce an enhancement in W501 fluorescence without hydrolysis. Previous studies with rabbit skeletal myosin were ambiguous in this respect because the greater enhancement induced by AMP·PNP compared with ADP could be a consequence of the slightly different conformations of the open state (equivalent to M*·ADP in eq 1). However with the Dd W501+ construct, this open binary complex is characterized by a quench in fluorescence for both the ADP and AMP·PNP induced states and therefore is more readily distinguished from any subsequent enhancement. The kinetic scheme for Dd myosin may therefore be modified from eq 2 to indicate the sensitivity of W501 to the different conformational states

$$\mathrm{M + ATP} \overset{1}{\rightleftharpoons} \mathrm{M.ATP} \overset{2}{\rightleftharpoons} \underset{\text{Open}}{\mathrm{M\dagger.ATP}} \overset{3a}{\rightleftharpoons} \underset{\text{Closed}}{\mathrm{M^{*}.ATP}} \overset{3b}{\rightleftharpoons} \underset{\text{Closed}}{\mathrm{M^{*}.ADP.Pi}} \overset{4}{\rightleftharpoons} \underset{\text{release}}{\text{Product}} \quad (5)$$

where the daggar (†) represents the quench and the asterisk (*) represents the enhancement sensed by the conserved W501 tryptophan. In this scheme, the first step represents a collision complex, the second step is an effectively irreversible isomerization, while the open-closed transitions (step 3a) and hydrolysis (step 3b) are freely reversible and kinetically coupled. According to the Geeves and Holmes (*9*) model, K_{3a} represents a rapid but unfavorable equilibrium for the open-closed transition (cf. K_{3a} estimated to be 0.2 from our results with AMP·PNP at 20 °C), which is offset by a favorable hydrolysis reaction ($K_{3b} \geq 10$ for ATP). The overall equilibrium for the combined transition is ≥2 and gives rise to a P_i burst amplitude of ≥0.67 mol P_i/mol motor domain. A consequence of this mechanism is that the M*·ATP state remains at a low concentration under most solution conditions (since k_{-3a} and k_{3b} are greater than k_{3a}) and, therefore, the open-closed transition and hydrolysis step appear almost coincident with an observed rate constant of about 30 s^{-1} at saturating [ATP]. In the limit, where the M*·ATP state is of negligible concentration, it is impossible to distinguish between a one and two-step mechanism by rapid-mixing methods. In any event, M*ATP would form rapidly ($k_{-3a} + k_{3b} \gg 100\ s^{-1}$) and hence any small initial enhancement phase would be practically coincident with, and hence nullify, the quench associated with M†·ATP formation so that neither amplitude could be extracted from the fluorescence profile. Perturbation methods may offer insight into this problem. We have observed additional transients that may be related to step3a in temperature jump transients (Málnási-Csizmadia and Bagshaw, unpublished observations). Alternatively, the small discrepancy between the rate constant for the fluorescence enhancement and the hydrolysis reaction measured in the experiment described in Figure 10a could be a reflection of a more significant contribution of M*·ATP to the fluorescence signal as would occur if $k_{3a} \approx k_{3b}$. However, systematic errors in the quenched-flow data preclude a rigorous conclusion. At this stage, we regard the potential for AMP·PNP to give rise to an enhanced W501 fluorescent state as the key evidence for existence of such a closed nucleoside triphosphate-state without the need for hydrolysis.

The overall equilibrium of step 3 is readily reversible and would require that both substeps are also reversible. In

particular, the equilibrium constant K_{3a} appears very temperature sensitive so that, at low temperatures, the open state is even more favored and this will reduce the overall P_i burst amplitude (*28*). From the data obtained with AMP·PNP (Figure 7), the open-closed transition is a very endothermic reaction ($\Delta H_o \approx +94$ kJ mol^{-1}) and accompanied by an increase in entropy ($\Delta S_o \approx 0.3$ kJ mol^{-1} K^{-1}) which together give a small free-energy change at 20° C ($\Delta G_o = +4$ kJ mol^{-1}). Previous measurements of the enthalpy of ATP hydrolysis in the active site have given ΔH_o values of +64 kJ mol^{-1} (*29*), but this would represent the combined open-closed transition and hydrolysis steps. It appears therefore that the hydrolysis step (3b), when resolved from the preceding transition (3a), has a $\Delta H_o \approx -30$ kJ mol^{-1}, more similar to that of the overall enthalpy change for ATP hydrolysis (−20 kJ mol^{-1}; ref *29*), although the ΔG_o remains relatively small. Temperature and pressure-jump experiments are in progress to explore further the kinetics of the open-closed transition. In this regard the M·ADP·BeF_3 appears a useful complex to examine because the equilibrium is poised between the open and closed states at ambient temperatures.

ATPγS and AMP·PNP induce the open state in a crystal, which is in accord with $K_{3a} < 1$, particularly at the low temperatures employed for crystal growth (*30*). However, it is not surprising that the same nucleotide can induce different crystal states of the motor domain (e.g., M·ADP·BeF_3 has been observed in both open and closed forms; refs *5* and *7*) given the low energy barrier associated with step 3a. Similarly, it is clear that the reverse transition, in itself, cannot correspond to the power stroke of the cross-bridge cycle. Only step 2 in the myosin mechanism has sufficient free energy to drive actomyosin dissociation (*3*). The equivalent step in the presence of actin involves reversal of the so-called A-state to R-state transition that is distinct from the open-closed transition at the nucleotide site (*9*). It might be envisaged that actin causes a further conformational change that introduces pawl into the molecular machinery, so that the freely reversible lever arm swing of the dissociated motor becomes much less reversible and the motor can maintain a force.

Myosins lacking the equivalent of W113 and W131 in skeletal myosin generally show no tryptophan fluorescence enhancement on binding ADP. Thus, there appears little tendency for ADP to induce the closed state. An exception is regulated scallop myosin in the absence of Ca^{2+} (*31*), where ADP possibly becomes trapped in an M*·ADP like-state which perturbs W507 (equivalent to Dd W501). Recently, Yengo at al. (*17*) reported a related mutagenesis study in a smooth muscle myosin where a single tryptophan mutant W512-MDE (equivalent to Dd W501+) was constructed. This mutant showed an enhanced fluorescence both in the steady-state nucleotide complex as well as with ADP. Again this suggests that ADP is capable of inducing the closed state to a limited extent and may be related to the particular properties of this myosin in showing ADP dependent structural changes detected at the level of electron microscopy (*32*).

The W501 side chain was not resolved in the either of the original Dd M·ADP·BeF_x (open) or Dd M·ADP·AlF_4 (closed) crystal structures (*5*). Of the open Dd structures published to date, W501 is only resolved in the dinitrophenyl aminoethyl diphosphate BeFx complex where its side chain is exposed to solvent (*33*). In contrast, W501 points into a hydrophobic region adjacent to the converter domain (Figure 1) in the Dd M*·ADP·Vi (closed) complex (*6*). The equivalent tryptophan residue W510 is resolved in the open skeletal myosin structure (nucleotide-free but sulfate bound) and is more exposed than that of the closed state (*34*), while a fourth orientation is seen in the novel scallop myosin·ADP structure (*8*). Interestingly in the latter case, the tryptophan is sandwiched between two charged basic residues that have the potential to quench tryptophan fluorescence (*34*). The M†·ADP state characterized here is the first clear case of a conformation with reduced fluorescence specifically associated with W501 and indicates that the nucleotide-free state and nucleotide-bound open states have different conformations in the relay region. The W501 residue (or equivalent) appears to be very dynamic in the crystal structures and, where resolved, no single orientation has been determined in the open structures. On the other hand, in the closed structures, the W501 or equivalent side chain, is internal (*6*, *7*). Time-resolved fluorescence anisotropy measurements are in progress to test this conclusion. Interpretation of these measurements is much simpler in a single tryptophan protein, such as W501+, where the signal can be uniquely assigned and energy transfer between tryptophan residues (a mechanism for depolarization) is prevented (*23*). It is likely that tryptophan mutants will continue to yield detailed information about myosin structure and function and build on the pioneering studies of Morita (*36*) reported over 30 years ago.

ACKNOWLEDGMENT

We are grateful to the Dr. Mark Taylor and Mrs. Nina Bhanji for assistance with the quenched-flow measurements.

REFERENCES

1. Werber, M. M., Szent-Györgyi, A. G., and Fasman, G. D. (1972) *Biochemistry 11*, 2872−2883.
2. Bagshaw, C. R., Eccleston, J. F., Trentham, D. R., Yates, D. W., and Goody, R. S. (1972) *Cold Spring Harbor Symp. Quantum Biol. 37*, 127−135.
3. Bagshaw, C. R., Eccleston, J. F., Eckstein, F., Goody, R. S., Gutfreund, H., and Trentham, D. R. (1974) *Biochem. J. 141*, 351−364.
4. Johnson, K. A., and Taylor, E. W. (1978) *Biochemistry 17*, 3432−3442.
5. Fisher, A. J., Smith, C. A., Thoden, J., Smith, R., Sutoh, K., Holden, H. M., and Rayment, I. (1995) *Biochemistry 34*, 8960−8972.
6. Smith, C. A., and Rayment, I. (1996) *Biochemistry 35*, 5404−5417.
7. Dominguez, R., Freyzon, Y., Trybus, K. M., and Cohen, C. (1998) *Cell 94*, 559−571.
8. Houdusse, A., Kalabokis, V. N., Himmel, D., Szent-Györgyi, A. G., and Cohen, C. (1999) *Cell 97*, 459−470.
9. Geeves, M. A., and Holmes, K. C. (1999) *Annu. Rev. Biochem.* 68, 687−728.
10. Ritchie. M. D., Geeves, M. A., Woodward, S. K. A., and Manstein, D. J. (1993) *Proc. Natl. Acad. Sci. U.S.A. 90*, 8619−8623.
11. Kuhlman, P. A., and Bagshaw, C. R. (1998) *J. Muscle Res. Cell Motil. 19*, 491−504.
12. Hiratsuka, T. (1992) *J. Biol. Chem. 267*, 14949−14954.
13. Park, S., Ajtai, K., and Burghardt, T. P. (1997) *Biochemistry 36*, 3368−3372.
14. Batra, R., and Manstein, D. J. (1999) *Biol. Chem. 380*, 1017−1023.

15. Yengo, C. M., Fagnant, P. M., Chrin, L., Rovner, A. S., and Berger, C. L. (1998) *Proc. Natl. Acad. Sci. U.S.A. 95*, 12944−12949.
16. Yengo, C. M., Chrin, L., Rovner, A. S., and Berger, C. L. (1999) *Biochemistry 38*, 14515−14523.
17. Yengo, C. M., Chrin, L., Rovner, A. S., and Berger, C. L. (2000) *Biophys. J. 78*, 243a.
18. Kurzawa, S. E., Manstein, D. J., and Geeves, M. A. (1997) *Biochemistry 36*, 317−323.
19. Manstein, D. J., Schuster, H.-P., Morandini, P., and Hunt, D. M. (1995) *Gene 162*, 129−134.
20. Manstein, D. J., and Hunt, D. M. (1995) *J. Muscle. Res. Cell Motil. 16*, 325−332.
21. Trentham, D. R., Bardsley, R. G., Eccleston, J. F., and Weeds, A. G. (1972) *Biochem. J. 126*, 635−644.
22. Eccleston, J. F., Dix, D. B., and Thompson, R. C. (1985) *J. Biol. Chem. 260*, 16237−16241.
23. Lakowicz, J. R. (1999) *Principles of Fluorescence Spectroscopy*, 2nd ed., Kluwer Academic, New York.
24. Batra, R, Geeves, M., and Manstein, D. J. (1999) *Biochemistry 38*, 6126−6134.
25. Sleep, J. A., Trybus, K. M., Johnson, K. A., and Taylor, E. W. (1981) *J. Muscle Res. Cell Motil. 2*, 373−399.
26. Sasaki, N., Shimada, T., and Sutoh, K. (1998) *J. Biol. Chem. 273*, 20334−20340.
27. Suzuki, Y., Yasunaga, T., Ohkura, R., Wakabayashi, T., and Sutoh, K. (1998) *Nature 396*, 380−383.
28. Taylor, E. W. (1977) *Biochemistry 16*, 732−740.
29. Millar, N. C., Howarth, J. V., and Gutfreund, H. (1987) *Biochem. J. 248*, 683−690.
30. Gulick, A. M., Bauer, C. B., Thoden, J. B., and Rayment, I. (1997) *Biochemistry 36*, 11619−11628.
31. Jackson, A. P., and Bagshaw, C. R. (1988) *Biochem. J. 251*, 515−526.
32. Whittaker, M., Wilson-Kubalek, E. M., Smith, J. E., Faust, L., Milligan, R. A., and Sweeney, H. L. (1995) *Nature 378*, 748−751.
33. Gulick, A, M,. Bauer, C. B., Thoden, J. B., Pate, E., Yount, R. G., and Rayment, I. (2000) *J. Biol. Chem. 275*, 398−408.
34. Rayment, I., Rypniewski, W. R., Schmidt-Bäse, K., Smith, R., Tomchick, D. R., Benning, M. M., Winkelmann, D. A., Wesenberg, G., and Holden, H. M. (1993) *Science 261*, 50−58.
35. Bivi, D. B., Kubota, S., Pearlstein, R., and Morales, M. F. (1993) *Proc. Natl. Acad. Sci. U.S.A. 90*, 6791−6795.
36. Morita, F. (1967) *J. Biol. Chem. 242*, 4501−4506.

BI001125J